

## Inter-annual variability of total ozone deduced from GOME and its relation to observed El Nino of 1997–1998

Sudipta Sarkar and Ramesh P. Singh\*

Department of Civil Engineering, Indian Institute of Technology-Kanpur, Kanpur 208 016, India

The Global Ozone Monitoring Experiment (GOME), a passive imaging spectrometer on-board ERS-2 satellite was launched in July 1995. This sensor measures the radiances in the visible and ultraviolet range. From the measured radiances the total ozone concentrations have been deduced globally. The total ozone concentrations over the Indian sub-continent have been extracted for the period 1996–1999 from the global data set. The overall trend of the monthly mean column ozone over Indian sub-continent is found to be decreasing for the latitude range 28°N–42°N while for the latitude range 6°N–26°N it is more or less the same. The small yearly data set affirms the decreasing trend that has been reported by earlier workers in the northern mid to high latitudes. Further, our detailed analysis shows the effect of the El Nino during 1997–1998 in the total ozone concentrations.

DUE to increasing urbanization and industrialization the chemical composition of the atmosphere is changing on a global scale. In the changing scenario, ozone plays a central role in tropospheric and stratospheric chemistry. The global trend in total ozone column is found to decline<sup>1–3</sup> at the mid latitudes of the Northern Hemisphere during the late winter since 1978. Efforts have been made to find out the extent and type of effect due to climatic phenomena such as El Nino and Southern Oscillations<sup>4</sup>. In this article, we have studied the annual variability of total ozone concentration and the possible effects of El Nino over the Indian sub-continent.

The Global Ozone Monitoring Experiment (GOME) measures the back-scattered earth radiance and solar irradiance in UV/visible wavelength (237 nm to 794 nm) with a spectral resolution of 0.17–33 nm. The spectrum is split into four spectral channels, each recorded by a photodiode array. The total ground coverage is obtained within 3 days at the equator by a 960 km across track swath (4.5 sec forward scan, 1.5 sec back scan) with a ground resolution of 40 × 320 km<sup>2</sup>.

In the present study we have used four years of GOME data (January 1996–October 1999) of the Indian sub-continent which have been extracted from the global data set. For the present study, two latitude ranges (lower latitude 6°N–26°N and mid latitude 28°N–42°N) have been considered over the Indian sub-continent and the monthly mean ozone concentrations have been deduced from the

daily measurements. Time series plots for the two latitude ranges are shown with a linear regression model (Figure 1).

Figure 1 *a* shows variations of total ozone column for the middle latitudes (28°N–42°N) during 1996–99. The high values are seen during winter (January–March) over the Northern Hemisphere with the highest value reached around February–March of each year. This is seen to decrease with the start of spring and reach a minimum value during June and July of every year. The overall trend is found to be decreasing which is similar to the declining trend<sup>2–3</sup> found over the middle latitudes of the

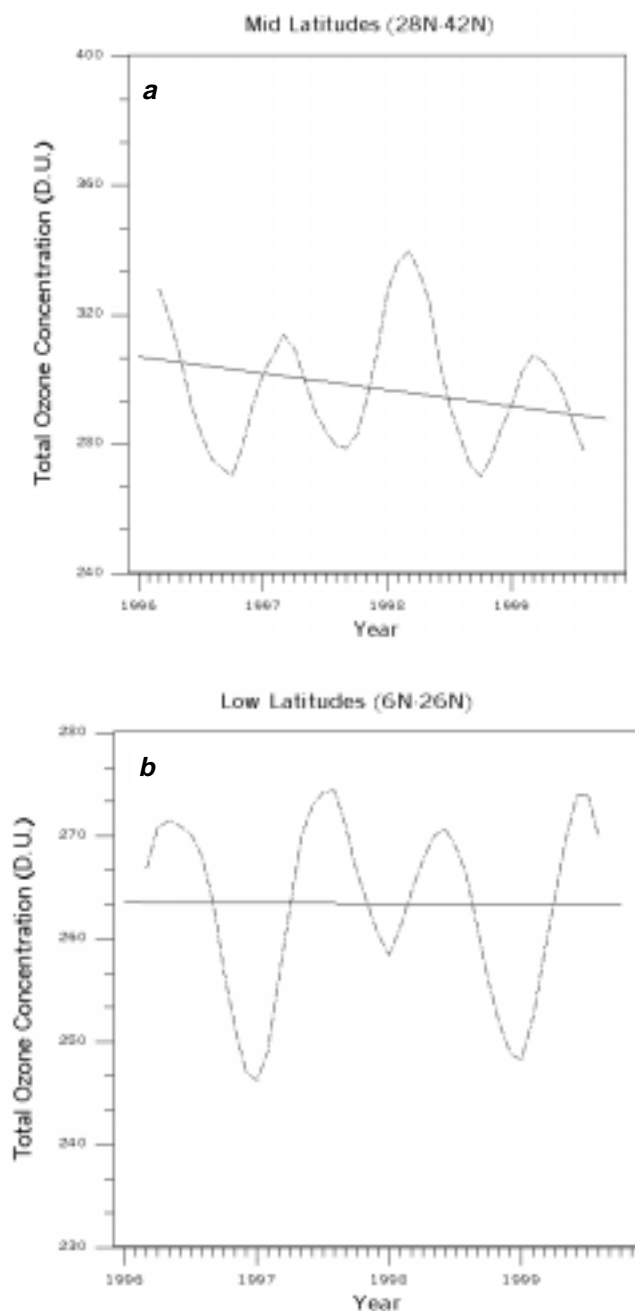


Figure 1. Variations of total ozone during 1996–99 for *a*, middle latitudes (28°N–42°N); and *b*, lower latitudes (6°N–26°N).

\*For correspondence. (e-mail: ramesh@iitk.ac.in)

entire Northern Hemisphere. However, the declining trend may be due to meridional mixing of chemically disturbed air from the Arctic polar vortex because of cooler springs in the present decade<sup>5</sup>. A similar time series plot for the lower latitude zone (Figure 1 *b*) produces no appreciable trend. Chakrabarty *et al.*<sup>6</sup> using six ground stations measured the ozone data for a longer period. They recently found an increasing trend for four stations, Kodaikanal, Ahmedabad, New Delhi and Srinagar, a decreasing trend for the Varanasi station and no trend for the Pune station. These stations are mostly located over the lower latitudes (6°N–26°N) with the exception of Srinagar and New Delhi and thus may not reflect the decreasing trend, which is more pronounced in the middle to higher latitudes. Incidentally, Kundu *et al.*<sup>7</sup> have found a negative trend in Srinagar ( $-0.260 \pm 0.032\%$  per year). Moreover, Chakrabarty *et al.*<sup>6</sup> have worked with a very large data set, for

the period of 1951 to 1996, due to which the decreasing trend over the recent years may have been overshadowed by the larger increasing trend for the previous years.

The seasonal variations during winter and summer seasons are shown during 1996–1999 for the two latitude zones (Figure 2). The seasonal variations for mid (Figure 2 *a*) and low latitude zones (Figure 2 *b*) show contrasting trend. In the mid latitudes, the total ozone concentration for winter is found to show continuously higher values compared to summer while in the lower latitude zones the ozone concentration is higher during summer compared to winter. This agrees well with earlier observations<sup>1–3,6</sup>, which is likely due to the change in intensity of the planetary waves from winter to summer.

The monthly variations for each year (1996–1998) over the Indian sub-continent (Figure 3 *a–d*) show most of the abrupt fluctuations towards the middle latitude. Such fluctuations reduce towards the equator. Further, a close analysis of Figures 1 *a* and 3 *a–d* shows a peak of total ozone during 1998. In Figure 1 *a* much higher peak is seen, centred during March 1998, whereas the monthly mean ozone value exceeds the four years average by 10%. Figure 3 *a–d* supports this and reveals an overall higher anomalous pattern during December 1997 and June 1998 (Figures 3 *b–c*). The mean total ozone value for this period (January 1998–June 1998) is 9.6% higher than the mean of a similar period taken over four years.

The total ozone concentration for the winter of 1998 (Figure 2 *a*) shows higher values compared to the winter of 1996–1997 and 1999, an anomaly against the trend set by the gradual decrease from 1996 to 1997 and from 1997 to 1999. This anomalous increase in the total ozone concentration for the period from January 1998 to April, June 1998 though not very prominent, is still manifested in the low latitude zone as shown in Figures 1 *b* and 2 *b*. The fluctuation from winter to summer is less in 1998 compared to that during 1997 and 1999 owing to less significant decrease in the winter of 1998.

The extent of this jump in total ozone can be seen in Figure 4 which shows the distribution of ozone concentrations in Dobson Unit during 1996–1999 for the month of March. A comparative study of the figures reveals a general downward shift in March 1998, of the higher total ozone concentration bands, towards lower latitudes over the Indian sub-continent. The bands are also seen to be more closely spaced with a greater gradient towards the middle to high latitudes over the Indian sub-continent. A similar behaviour is also seen for the months of January and February 1998 (not shown).

The migration of column ozone bands coincides with a warmer than normal temperature over the Indian sub-continent for January to March 1998. The January to July 1998 mean temperature for the Indian sub-continent is found to be 1–3°C higher<sup>8</sup> compared to January to July 1997. This fits well with the observed higher global surface temperature data for January to March 1998.

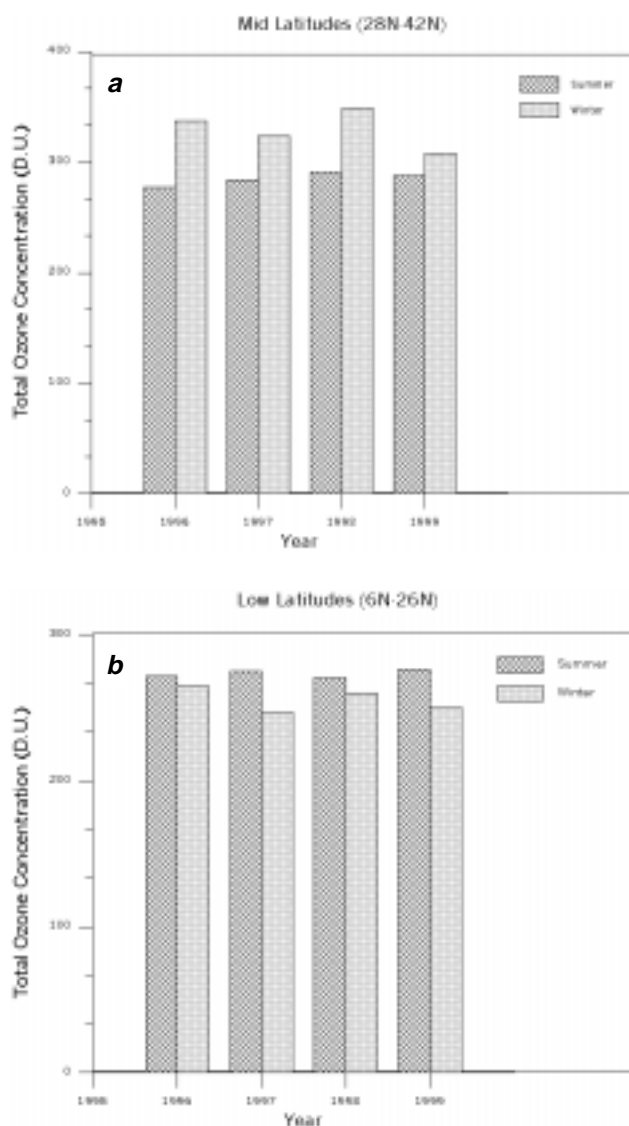


**Figure 2.** Seasonal variations during 1996–1999 for *a*, middle latitudes (28°N–42°N); and *b*, lower latitudes (6°N–26°N).

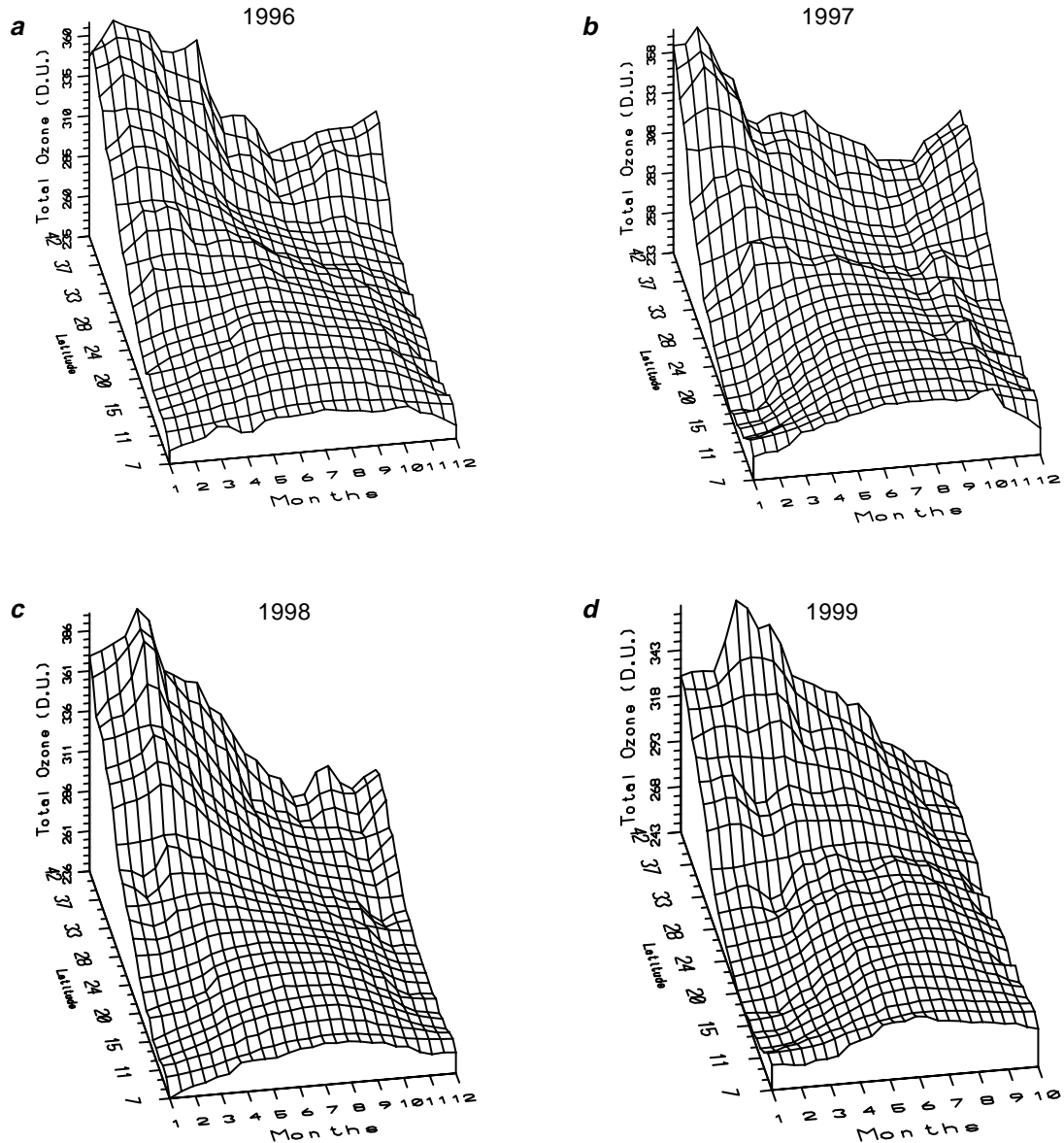


**Figure 3.** Surfaces showing monthly variations of total ozone concentration for *a*, 1996; *b*, 1997; *c*, 1998; and *d*, 1999 at location 78.3°E.

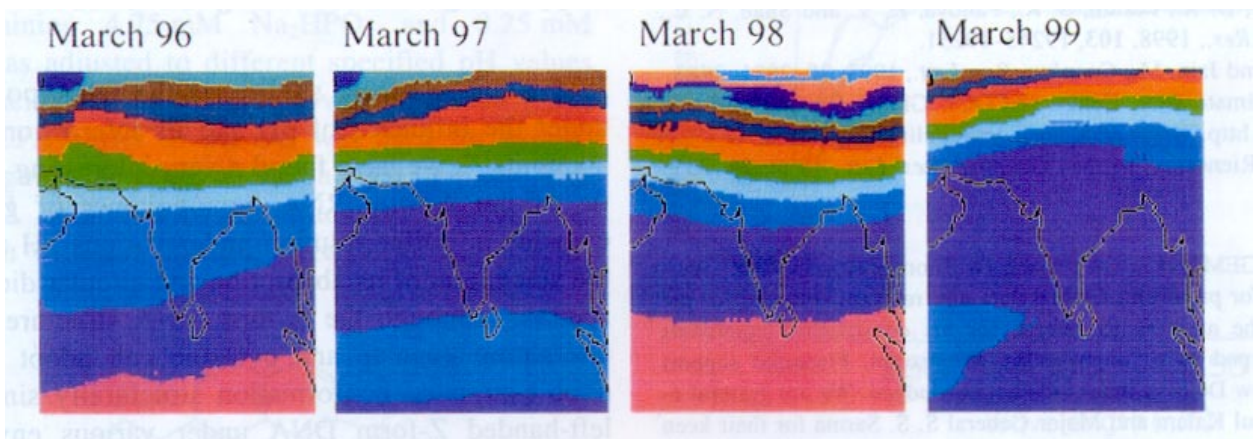


**Figure 4.** Yearly (1996–1999) distribution of ozone concentration over the Indian sub-continent for the month of March.

The sea-surface temperature (SST) over equatorial Indian ocean has also been found higher during the first few months of 1998. By March 1998, nearly the entire Indian ocean shows considerably warmer SST than normal<sup>9</sup>. This is largely due to the strong El Nino<sup>9</sup> event of 1997–1998. At the same time in the higher latitudes beyond the Indian sub-continent, during January and July 1998 the mean temperature is found to be 1–4°C lower<sup>8</sup> than that observed during January and July 1997. Hence, we infer that cooler higher latitudes along with warmer lower, lower–middle latitudes may have resulted in a more pronounced temperature gradient. This in turn may have led to modulation of Hadley cell and stronger stratospheric transfer of ozone (Brewer Dobson circulation) from lower to higher latitudes. Thus the observed shift in the total column ozone bands over the Indian sub-continent may be attributed to the temperature anomaly caused by the strong El Nino of 1997–98.

*Note added in proof:*

The total ozone concentration deduced from GOME shows a negative trend for mid latitudes, however, the trend is positive for almost all the Indian stations which is confirmed by TOMS satellite and total ozone ground data observed at Indian stations (data available from IMD, Pune). This ruled out any health hazard at least on the Indian continent. The latest findings will be communicated soon.

1. Stolarski, R. S., Bloomfield, P. and McPeters, R. D., *Geophys. Res. Lett.*, 1991, **18**, 1015–1018.
2. Hollandsworth, S. M., McPeters, R. D., Flynn, L. E., Planet, W., Miller, A. J. and Chandra, S., *Geophys. Res. Lett.*, 1995, **22**, 905–908.
3. McPeters, R. D., Hollandsworth, S. M., Flynn, L. E., Herman, J. R. and Seftor, C. J., *Geophys. Res. Lett.*, 1996, **23**, 3699–3702.
4. Langford, A. O., O'Leary, T. J., Masters, C. D., Aikin, K. C. and Proffitt, M. H., *Geophys. Res. Lett.*, 1998, **25**, 2667–2670.
5. Bojkov, R. D., Balis, D. S. and Zerefos, C. S., *Meteorol. Atmos. Phys.*, 1998, **69**, 119–135.
6. Chakrabarty, D. K., Peshin, S. K., Pandya, K. V. and Shah, N. C., *J. Geophys. Res.*, 1998, **103**, 19245–19251.
7. Kundu, N. and Jain, M., *Geophys. Res. Lett.*, 1993, **20**, 2881–2883.
8. National Climate Data Centre (NCDC), Global Climate Bulletin, 1998, 1999. <http://www.ncdc.noaa.gov/ol/climate/research>.
9. Yu, L. and Rienecker, M. M., *Geophys. Res. Lett.*, 1999, **26**, 735–738.

**ACKNOWLEDGEMENTS.** We thank Dr Thomas Koenig DLR, Wesling, Germany for providing GOME data and relevant software for the analysis, and the anonymous referee for his constructive comments which have helped us to improve the manuscript. Financial support from DTSR, New Delhi is thankfully acknowledged. We are grateful to Dr A. P. J. Abdul Kalam and Major General S. S. Sarma for their keen interest in the present work.

Received 5 January 2000; revised accepted 4 May 2000

## Interaction of sanguinarine with A-form and protonated form of ribonucleic acid structures: Spectroscopic, viscometric and thermodynamic studies

S. Das, Anamika Banerjee, Anjana Sen and M. Maiti\*

Biophysical Chemistry Laboratory, Indian Institute of Chemical Biology, Jadavpur, Calcutta 700 032, India

The interaction of sanguinarine with the A-form and the protonated form of poly(rG).poly(rC) has been investigated using a combination of spectrophotometric, spectrofluorimetric, circular dichroic (CD), viscometric and thermodynamic studies. The formation of the two forms of this structure has been confirmed from UV-absorption and CD spectral characteristics. The binding of sanguinarine to both the A-form and the protonated form RNA structures is characterized by the typical hypochromic and bathochromic effects in the absorption spectrum, quenching of fluorescence intensity, decrease in fluorescence quantum yield of the alkaloid, an increase in fluorescence polarization anisotropy and perturbation in the CD spectrum. Scatchard plots obtained from spectrophotometric and spectrofluorimetric analyses show that sanguinarine binds to both the structures in a non-cooperative manner. The binding parameters, according to an excluded site model, indicate a relatively high affinity of the alkaloid binding to the A-form structure than to the protonated form structure. Viscometric studies demonstrate that there is no increase in the contour length of the sonicated A-form and the protonated form RNA structures upon binding to sanguinarine. Thermodynamic parameters as revealed from van't Hoff plot indicate that the RNA binding of the alkaloid is an exothermic process and it binds more tightly to the protonated form than the A-form structure. The intermolecular interaction of sanguinarine is characterized by negative enthalpy changes and positive entropy changes at the binding site of the two structures.

IN the course of our studies on the DNA polymorphism under the influence of pH and its interaction with plant alkaloids<sup>1–4</sup>, we have found a very interesting characteristic of the A-form RNA homopolymer of guanine and cytosine in buffer solution under various pH values from the standpoint of its absorption and circular dichroic (CD) spectra. Although the A-form RNA structure containing alternating guanine and cytosine can adopt left-handed double-stranded conformation structurally similar to the left-handed Z-form DNA under various environmental conditions<sup>5,6</sup>, not much information is known about the

\*For correspondence. (e-mail: mmaiti@iicb.res.in)

polymorphic structure of poly(rG).poly(rC) which is very stable and present in various genomes of RNA double-stranded viruses<sup>7-9</sup>. There is considerable interest in developing organic compounds that can interact with RNA of these viruses and exert antiviral activity. Though there have been a few detailed studies on the RNA-binding mode of organic compounds<sup>10-15</sup>, efforts have not been made to understand the RNA-alkaloid interactions. Recent studies have demonstrated that the broad structural diversity of RNA is crucial for recognizing small ligands, peptides and proteins<sup>16</sup>.

Sanguinarine (Figure 1), a benzophenanthridine plant alkaloid, has attracted recent attention for its diverse biological, photophysical, photochemical and DNA-binding properties<sup>17-32</sup>. We have demonstrated that (i) Sanguinarine (iminium form) binds to the B-form DNA structure by the mechanism of intercalation with high preference to GC base pairs<sup>22,24,31</sup>; (ii) It converts cooperatively the left handed Z-form and the left handed H<sup>L</sup>-form to bound right handed B-form structure<sup>4</sup>. The focus of our present study is to characterize the A-form poly(rG).poly(rC) and its protonated structure and its binding to sanguinarine in order to elucidate the mode and mechanism of binding of the alkaloid using various spectroscopic, viscometric and thermodynamic studies.

Sanguinarine chloride was obtained from Aldrich Chemical Co, Milwaukee, USA, and was used without further purification. The alkaloid solution was freshly prepared each day by dissolving appropriate amounts in acidic buffer and was always kept protected in the dark to prevent any light-induced changes. A molar extinction coefficient ( $\epsilon$ ) of 30,700 M<sup>-1</sup> cm<sup>-1</sup> at 327 nm in 0.1 N HCl was used for determining the concentration. The alkaloid obeyed Beer's law in the concentration range was used. Poly(rG).poly(rC) was purchased from Sigma Chemical Co, St. Louis, USA and was used as such. The concentration of poly(rG).poly(rC) in terms of nucleotide phosphate was estimated spectrophotometrically using known molar extinction coefficients ( $\epsilon$ ) 7700 M<sup>-1</sup> cm<sup>-1</sup> at 259 nm in buffer of neutral pH. Citrate-phosphate-EDTA (CPE) buffer containing 4.75 mM Na<sub>2</sub>HPO<sub>4</sub> and 0.25 mM Na<sub>2</sub>EDTA was adjusted to different specified pH values using citric acid. All the buffers provided constant [Na<sup>+</sup>] of 10 mM. CPE buffer of pH 5.2 was used for experiments as sanguinarine exists as the charged iminium form at this pH<sup>26,27</sup>. Formation of the protonated structure and its interaction with this alkaloid were performed in CPE

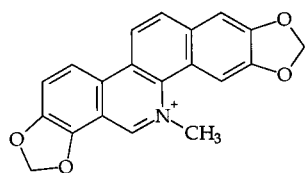


Figure 1. Chemical structure of sanguinarine.

buffer of pH 4.3. Analytical grade reagents and deionized triple distilled water were used throughout.

Absorbance and steady state fluorescence spectra of either sanguinarine alone or mixed with RNA were obtained using a Shimadzu UV-260 automatic recording double beam spectrophotometer and a Hitachi F-4010 spectrofluorimeter equipped with temperature controlling set-up as described earlier<sup>33-35</sup>. Spectroscopic titration data were used to construct Scatchard plot using McGhee and von Hippel equation<sup>36</sup> for a nonlinear, non-cooperative ligand binding system according to the following equation:

$$\frac{r}{C_f} = K'(1 - nr) \left[ \frac{(1 - nr)}{1 - (n-1)r} \right]^{(n-1)},$$

where  $K'$  is the binding constant to an isolated RNA binding site and  $n$  is the number of nucleotides occluded after binding of a single alkaloid molecule. The SCATPLOT program was used for obtaining the best fit to the theoretical line as described in Ray *et al.*<sup>37</sup>. Fluorescence quantum yield, Stern-Volmer quenching constant data and fluorescence polarization anisotropy were evaluated as reported earlier<sup>32-34</sup>. Thermal denaturation temperature ( $T_m$ ) of RNA structures was measured under appropriate solution condition as described previously<sup>33</sup>. The temperature was scanned at a heating rate of either 0.5°C/min or 1°C/min. CD measurements were carried out on a Jasco J-720 spectropolarimeter attached with a thermal programmer model PTC 343 as reported earlier<sup>4,35</sup>.

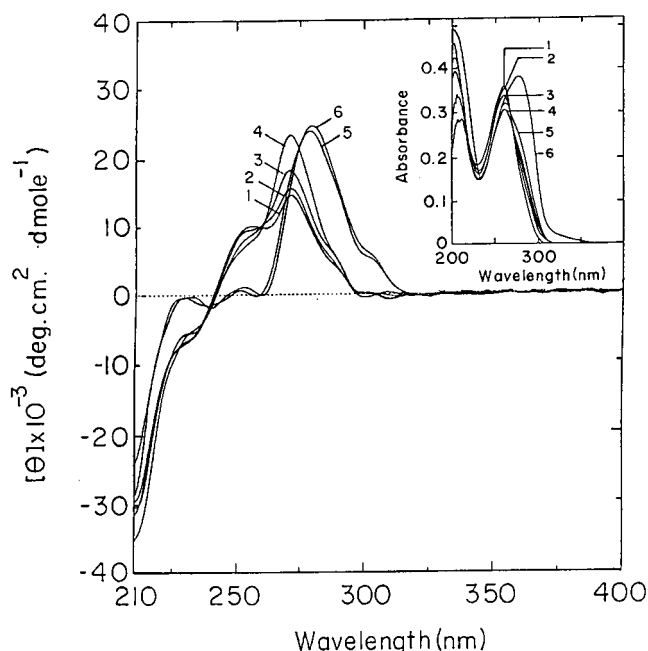


Figure 2. Influence of pH on the CD spectrum of poly(rG).poly(rC) (30.33  $\mu$ M) in 10 mM CPE buffer at 20°C. Curves 1-6 represent pH values 7.0, 5.40, 4.70, 4.30, 2.90 and 2.44, respectively. (Inset) UV spectral changes of poly(rG).poly(rC) (45.95  $\mu$ M) in the buffer of the above pH values.

The RNA duplex was sonicated in a LABSONIC-2000 sonicator (B Braun, Swiss) by using a needle probe of 4 mm diameter. The size of the polymer was found to be  $260 \pm 60$  bp as determined from viscometric measurements which were performed using Cannon Manning Type 75 semi-micro viscometer mounted vertically in a constant temperature bath (Cannon Instrument Co., State College, PA, USA) maintained at  $20 \pm 0.1^\circ\text{C}$ . The flow times of RNA alone and RNA-alkaloid complexes were measured by an electronic stop-watch (Casio stop-watch, Model HS-30 W, Japan) with an accuracy of 0.01 sec and elongation of the length of the RNA structure was determined as described earlier<sup>22,33</sup>.

Temperature-dependent spectrophotometric and spectrofluorimetric titrations were performed for the sanguinarine-RNA complexation to estimate the thermodynamic parameters. The analysis of van't Hoff plot ( $\ln K'$  vs  $1/T$ ) obtained over the temperature range of the study enabled the calculation of  $\Delta H^\circ$ , as the gradient equal to  $-\Delta H^\circ/R$ .  $\Delta G^\circ$  and  $\Delta S^\circ$  were calculated from the relationships  $\Delta G^\circ = -RT \ln K'$  and  $\Delta G^\circ = \Delta H^\circ - T\Delta S^\circ$  as described in Nandi *et al.*<sup>33</sup>.

The UV absorbance and CD changes in the A-form poly(rG).poly(rC) under the influence of pH at  $20^\circ\text{C}$  are depicted in Figure 2. The typical A-form CD spectrum of poly(rG).poly(rC) at pH 7.0 undergoes changes which involve essentially an increase in intensity of the CD band at around 271 nm and the appearance of an isoelliptic point at around 258 nm up to pH value of 4.3. Molar ellipticity of the characteristic maximum is increased from  $14,000 \text{ deg.cm}^2.\text{dmole}^{-1}$  to  $23,300 \text{ deg.cm}^2.\text{dmole}^{-1}$ . On further lowering of the pH of the medium, the spectrum obtained is red-shifted about 10 nm with departure from the isoelliptic point. The UV spectrum of this polymer at pH 7.0 has a band centred at 260 nm and changes associated with this spectrum at different pH values are shown in the inset of Figure 2. The absorption band essentially undergoes hypochromic and bathochromic shift with decreasing pH of the medium. These changes are clearly distinct with an isosbestic point at 272 nm. Thereafter below pH 3.0, duplex polymer starts acid denaturation as is evident from the enhancement of absorbance at 285 nm and the departure of the spectrum from the isosbestic point. Both UV and CD data clearly show that before acid denaturation the polymer has undergone a conformational change from its A-form structure, forming an equilibrium between the A-form and the protonated form structures. It is worth noting that UV and CD spectral changes are completely reversible when the polymer solution is transformed to neutral pH indicating a duplex nature of the protonated structure. The stability of this protonated structure is further confirmed from thermal melting studies. We have found that neither the A-form nor the protonated form can undergo helix to coil transition up to a temperature of  $95^\circ\text{C}$ , indicating that both the structures are very thermostable.

The interaction of sanguinarine with the two forms of poly(rG).poly(rC) was monitored using absorption spectroscopy in the 300–550 nm range. The effect of progressively increasing the concentration of the A-form and the protonated form on the absorption spectrum of sanguinarine is shown in Figure 3 *a* and *b*, respectively. The sanguinarine absorption spectrum shifts to a longer wavelength and displays large hypochromicity on binding to both the structures. Three isosbestic points at 352, 368 and 495 nm in all the cases indicate the equilibrium between the bound and the free alkaloid molecules. The values of  $K'$  and  $n$  obtained from spectrophotometric titration data are presented in Table 1. The results show a relatively high affinity of sanguinarine binding to the A-form structure than to the protonated structure.

Sanguinarine shows emission maximum at 577 nm in the wavelength range 500–650 nm when excited at 475 nm. With increasing concentration of both the forms of RNA,

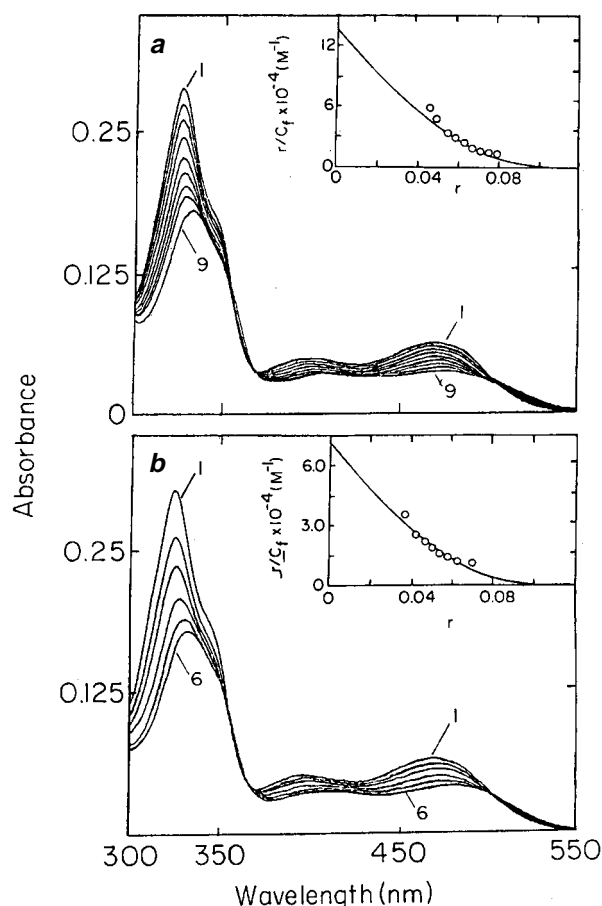


**Figure 3.** Representative absorption spectrum of sanguinarine treated with A-form and protonated form of poly(rG).poly(rC). *a*, Sanguinarine (9.41  $\mu\text{M}$ , curve 1) treated with 15.7, 29.5, 53.0, 82.3, 117.4, 158, 203.9 and 227.8  $\mu\text{M}$  (curves 2–9) of A-form of poly(rG).poly(rC) in 10 mM CPE buffer, pH 5.2 at  $20^\circ\text{C}$ ; *b*, Sanguinarine (9.93  $\mu\text{M}$ , curve 1) treated with 49.8, 83.7, 164.5, 251.2 and 317.3  $\mu\text{M}$  (curves 2–6) of protonated form of poly(rG).poly(rC) in 10 mM CPE buffer, pH 4.3 at  $15^\circ\text{C}$ . (Inset) Scatchard plot for the complexation of sanguinarine with A-form (*a*) and protonated form (*b*) of poly(rG).poly(rC).

**Table 1.** Binding parameters for the interaction of sanguinarine with A-form and protonated form of poly(rG).poly(rC) structures<sup>a</sup>

Parameters	Methods	Values	
		A-form RNA	Protonated form RNA
$K'$ , the intrinsic binding constant ( $M^{-1}$ )	Spectrophotometry	$(13.5 \pm 0.3) \times 10^4$	$(7.0 \pm 0.2) \times 10^4$
	Spectrofluorimetry	$(13.0 \pm 0.4) \times 10^4$	$(7.2 \pm 0.3) \times 10^4$
$n$ , the number of nucleotides occluded	Spectrophotometry	$8.8 \pm 0.09$	$9.0 \pm 0.11$
	Spectrofluorimetry	$10.0 \pm 0.12$	$11.8 \pm 0.14$
$\phi/\phi_0^b$	Spectrofluorimetry	$0.30 \pm 0.03$	$0.39 \pm 0.04$
	Fluorescence polarization anisotropy <sup>c</sup>	$0.21 \pm 0.02$	$0.17 \pm 0.02$
$K_{SV}$ , Stern–Volmer quenching constant ( $M^{-1}$ ) <sup>d</sup>	Spectrofluorimetry	$(2.2 \pm 0.1) \times 10^4$	$(1.5 \pm 0.1) \times 10^4$

<sup>a</sup>Three determinations each. <sup>b</sup>Steady state fluorescence quantum yield ( $\phi$ ) was determined from the equation  $\phi_s = (F_s \epsilon_q C_q / F_q \epsilon_s C_s) 0.55$  as described earlier<sup>34</sup>, where  $s$  and  $q$  denote sample and quinine sulphate in 0.1 N  $H_2SO_4$  respectively;  $F$  denotes the integral area of fluorescence excitation at the same wavelength;  $\epsilon$  is at the wavelength of excitation and  $C$  represents the corresponding concentration;  $\phi/\phi_0$  denotes the relative quantum yield;  $P/D$  values of 50 for both the structures. <sup>c</sup>Data obtained at  $P/D$  value of 80 and 100 for A-form and protonated form of poly(rG).poly(rC), respectively. <sup>d</sup> $K_{SV}$  is the Stern–Volmer quenching constant determined from the equation  $I_0/I = 1 + K_{SV}[Q]$ . Where  $I_0$  and  $I$  are the fluorescence emission intensities in the absence and in the presence of a quencher  $[Q]$ .

a progressive quenching of fluorescence intensity accompanied by a gradual blue shift is observed. The fluorescence spectra of sanguinarine with the interaction of the A-form and the protonated form of poly(rG).poly(rC) are depicted in Figure 4 *a* and *b*, respectively. The decrease in absorbance at 327 nm and fluorescence intensity at 577 nm are used to express the data in the form of Scatchard plots. It has been found that fluorescence polarization anisotropy value increases considerably upon binding of sanguinarine to both the structures. The quantitative data on binding constants, quantum yield, Stern–Volmer quenching constant ( $K_{SV}$ ) and anisotropy values are presented in Table 1. The data obtained from two independent methods do not differ significantly in each case.

The changes in the CD spectra of the A-form and the protonated form of poly(rG).poly(rC) in the presence of sanguinarine are depicted in Figure 5 *a* and *b*, respectively. Figure 5 *a* shows that there is an increase in the ellipticity of the characteristic CD band at 270 nm of the A-form with increasing concentration of the alkaloid. An isoelliptic point is observed at around 249 nm. On addition of the alkaloid to the protonated form of RNA there is a red shift of the 270 nm peak and then increase in ellipticity of the peak is noted along with a sharp isoelliptic point at around 274 nm. Appearance of the isoelliptic point indicates an equilibrium between the alkaloid bound and the free polymer in each case. Such changes in the intrinsic CD generally represent conformational changes consequent to strong binding of small molecules between the base pairs of nucleic acids. Sanguinarine is an optically inactive molecule and it does not have any CD spectrum in the entire UV–VIS range. On binding to the A-form of RNA, sanguinarine acquires optical activity manifested by the appearance of a positive CD band in the 320–370 nm region, while no extrinsic CD is found on the interaction of sanguinarine with the protonated form, indi-

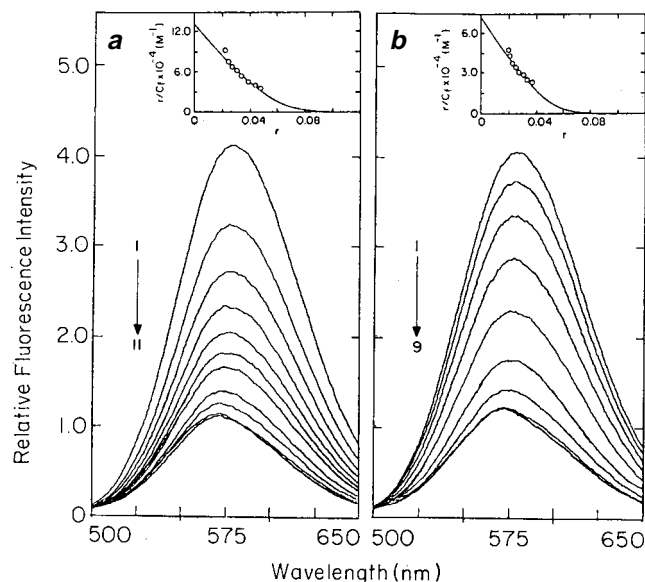


**Figure 4.** Representative fluorescence spectrum of sanguinarine (1.99  $\mu M$ , curve 1) treated with *a*, 12.1, 24.1, 36.2, 48.3, 60.4, 80.5, 100.6, 120.7, 128.8, and 140.8  $\mu M$  (curves 2–11) of A-form of poly(rG).poly(rC) in 10 mM CPE buffer, pH 5.2 at 20°C; *b*, 12.1, 24.1, 36.2, 48.3, 80.5, 100.6, 120.7 and 161.0  $\mu M$  (curves 2–9) of protonated form of poly(rG).poly(rC) in 10 mM CPE buffer, pH 4.3 at 15°C. (Inset) Scatchard plot for the complexation of sanguinarine with A-form (*a*) and protonated form (*b*) of poly(rG).poly(rC).

cating the absence of alkaloid–alkaloid asymmetric arrangement in this structure.

Several small molecules have been reported to interact with RNA duplexes in a reversible manner<sup>10–15</sup>. Tanious *et al.*<sup>13</sup> have shown that DAPI binds to poly(rA).poly(rU) by the mechanism of intercalation, while it binds strongly to the minor groove of DNA. The minor and major grooves of the A-form RNA duplexes, however, differ very significantly from those of the B-form DNA<sup>5</sup>. The

grooves of RNA and DNA have different steric characteristics, different chemical characteristics due to features, viz. the 2'-OH groups in the RNA minor groove and different relative molecular electrostatic potential<sup>5,38,39</sup>. Two phenanthridium derivatives, ethidium and propidium, have been reported to form intercalation complexes with RNA<sup>10-12</sup>. Elicpticine and proflavine have been shown to intercalate RNA structures<sup>15</sup>. Some unfused aromatic compounds have also been reported to bind RNA by the mechanism of intercalation<sup>15</sup>. Despite the differences in conformations between the double-stranded DNA and the double-stranded RNA structure<sup>5</sup>, sanguinarine on binding to both forms of RNA shows characteristic hypochromism and bathochromism of the absorption spectrum, quenching of steady state fluorescence intensity, decrease in quantum yield and perturbation in the CD spectrum. These behaviours are the same for the sanguinarine-DNA complexation<sup>22-25</sup>. The similarity in behaviour suggests a similarity in the mechanism of binding of sanguinarine to the RNA structure. The viscometric technique is a well-established method for investigating the extension of a DNA or RNA helix associated with intercalation<sup>12,22</sup>. The present study

demonstrates that there is no change in viscosity of the sonicated A-form and the protonated form of poly(rG).poly(rC) on complexation with sanguinarine. The data clearly indicate that sanguinarine does not intercalate to any of the two forms of RNA. It may bind to these RNA structures by some other mechanism, which could not be established from the present study.

It is known that thermodynamic and structural studies are mutually complementary and both are necessary for the complete elucidation of molecular details of the binding process for the delineation of the molecular interaction at the interaction site<sup>40,41</sup>. The results of spectrophotometric and spectrofluorimetric studies at various temperatures allowed us to thermodynamically characterize the mode of binding and to define the driving forces behind the binding process. It has been observed that value of binding constant decreases with increasing temperature in both the cases. The values of thermodynamic parameters evaluated from the van't Hoff plot (Figure 6) are presented in Table 2. Conceptually, thermodynamic parameters, enthalpy and entropy changes for the binding processes can be determined from the contributions of

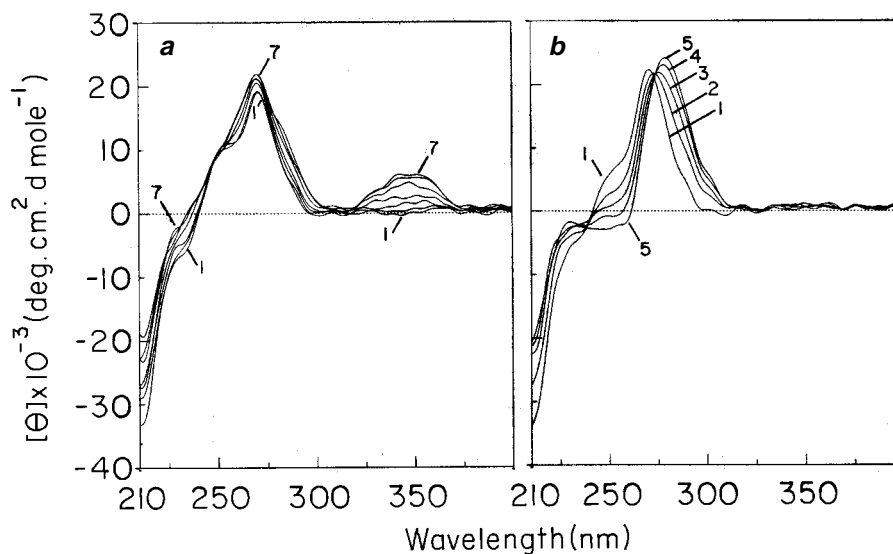


**Figure 5.** Representative CD spectra resulting from the interaction of sanguinarine with A-form and protonated form of poly(rG).poly(rC) (30.33  $\mu\text{M}$ ) at 20°C. **a**, Curves 1–7 denote A-form of poly(rG).poly(rC) treated with 0, 1.51, 4.03, 6.53, 9.02, 12.50 and 17.43  $\mu\text{M}$  of sanguinarine in 10 mM CPE buffer, pH 5.2; **b**, Curves 1–5 denote protonated form of poly(rG).poly(rC) treated with 0, 2.02, 4.03, 6.03 and 12.01  $\mu\text{M}$  of sanguinarine in 10 mM CPE buffer, pH 4.3. The expressed molar ellipticity is based on polynucleotide concentration.

**Table 2.** Thermodynamic parameters on the interaction of sanguinarine with A-form and protonated form of poly(rG).poly(rC)<sup>a</sup>

Method	A-form RNA			Protonated form RNA		
	$\Delta G_{20,c}^{\circ}$ (kcal mol <sup>-1</sup> )	$\Delta H^{\circ}$ (kcal mol <sup>-1</sup> )	$\Delta G_{20,c}^{\circ}$ (calK <sup>-1</sup> mol <sup>-1</sup> )	$\Delta S_{20,c}^{\circ}$ (kcal mol <sup>-1</sup> )	$\Delta H^{\circ}$ (kcal mol <sup>-1</sup> )	$\Delta S_{20,c}^{\circ}$ (calK <sup>-1</sup> mol <sup>-1</sup> )
Spectrophotometry	-6.92 ± 0.05	-3.64 ± 0.04	+11.17 ± 0.03	-6.44 ± 0.09	-5.11 ± 0.05	+4.61 ± 0.03
Spectrofluorimetry	-6.83 ± 0.03	-4.15 ± 0.05	+9.12 ± 0.03	-6.42 ± 0.04	-5.02 ± 0.02	+4.79 ± 0.04

<sup>a</sup>Three determinations each.

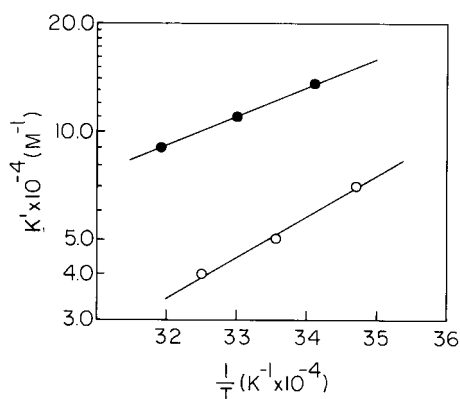


**Figure 6.** Representative van't Hoff plot for the complexation of sanguinarine with A-form (●) and protonated form (○) of poly(rG).poly(rC).

several factors at the binding site such as van der Waal's interactions, hydrophobic interactions, electrostatic interactions, conformational changes and ion release or change in hydration<sup>40-42</sup>. The possible contribution of negative enthalpy change for the binding process of sanguinarine to both the structures may be explained in terms of the van der Waal's stacking interactions, hydrophobic as well as weak electrostatic interactions, while the positive entropy changes are due to release of sodium ions and changes in hydration of RNA duplex structures. Thus, thermodynamic data reveal that the binding of sanguinarine is an exothermic process and the intermolecular interaction at the binding site of both the structures is characterized by negative enthalpy changes and positive entropy changes.

- Maiti, M. and Nandi, R., *Indian J. Biochem. Biophys.*, 1986, **23**, 322-325.
- Maiti, M. and Nandi, R., *Anal. Biochem.*, 1987, **164**, 68-71.
- Kumar, G. S. and Maiti, M., *J. Biomol. Struct. Dyn.*, 1994, **12**, 183-201.
- Das, S., Suresh Kumar, G. and Maiti, M., *Biophys. Chem.*, 1999, **76**, 199-218.
- Saenger, W., *Principles of Nucleic Acid Structure*, Springer-Verlag, New York, 1984.
- Hall, K., Kruz, P., Tinoco, I. Jr., Jovin, T. M. and van de Sande, J. H., *Nature*, 1984, **311**, 584-586.
- Brown, F., Newman, J., Scott, J., Porter, A., Frisby, D., Newton, C., Carey, N. and Fellner, P., *Nature*, 1974, **251**, 342-344.
- Rowlands, D. J., Harris, T. J. R. and Brown, F., *J. Virol.*, 1978, **26**, 335-343.
- Newton, S. E., Carroll, A. R., Campbell, R. O., Clarke, B. E. and Rowlands, D. J., *Gene*, 1985, **40**, 331-336.
- Bresloff, J. L. and Crothers, D. M., *Biochemistry*, 1981, **29**, 3547-3553.
- Babayan, Y., Manzini, G., Xodo, L. and Quadrioglio, F., *Nucleic Acids Res.*, 1987, **15**, 5803-5812.
- Waring, M. J., in *The Molecular Basis of Antibiotic Action* (eds Gale, E. F., Cundiffe, E., Reynolds, P. E., Richmond, M. H. and Waring, M. J.), Wiley, New York, 1981, 2nd edn, p. 287.

- Tanious, A. S., Veal, J. M., Buczak, H., Ratmeyer, L. S. and Wilson, W. D., *Biochemistry*, 1992, **31**, 3103-3112.
- Manzini, G., Xodo, L., Barcellona, M. L. and Quadrioglio, F., *Nucleic Acids Res.*, 1985, **13**, 8955-8967.
- Wilson, D. W., Ratmeyer, L., Zhao, M., Streckowski, L. and Boykin, D., *Biochemistry*, 1993, **32**, 4098-4194.
- Ramos, A., Gubser, C. C. and Varani, *Curr. Opin. Struct. Biol.*, 1997, **7**, 317-323.
- Preininger, V., in *The Alkaloids* (ed. Manske, R. H. F.), Academic Press, New York, 1975, vol. XV, p. 207.
- Nandi, R., Maiti, M., Chaudhuri, K., Mahato, S. B. and Bairagi, A. K., *Experientia*, 1983, **39**, 524-525.
- Kuo, C. L., Chou, C. C. and Yung, B. Y. M., *Cancer Lett.*, 1995, **93**, 193-200.
- Babich, H., Znckerbraun, H. L., Barber, I. B., Babich, S. B. and Borenfreund, E., *Pharmacol. Toxicol.*, 1996, **78**, 397-403.
- Wolff, J. and Knipling, L., *Biochemistry*, 1993, **32**, 13334-13339.
- Maiti, M., Nandi, R. and Chaudhuri, K., *FEBS Lett.*, 1982, **142**, 280-284.
- Maiti, M., Nandi, R. and Chaudhuri, K., *Indian J. Biochem. Biophys.*, 1984, **21**, 158-165.
- Maiti, M. and Nandi, R., *J. Biomol. Struct. Dyn.*, 1987, **5**, 159-175.
- Nandi, R. and Maiti, M., *Biochem. Pharmacol.*, 1985, **34**, 321-324.
- Maiti, M., Nandi, R. and Chaudhuri, K., *Photochem. Photobiol.*, 1983, **38**, 245-249.
- Das, A., Nandi, R. and Maiti, M., *Photochem. Photobiol.*, 1992, **56**, 311-317.
- Nandi, R., Chaudhuri, K. and Maiti, M., *Photochem. Photobiol.*, 1985, **42**, 497-503.
- Saran, A., Srivastava, S., Coutinho, E. and Maiti, M., *Indian J. Biochem. Biophys.*, 1995, **32**, 74-77.
- Maiti, M. and Chatterjee, A., *Curr. Sci.*, 1995, **68**, 734-736.
- Sen, A., Ray, A. and Maiti, M., *Biophys. Chem.*, 1996, **59**, 155-170.
- Sen, A. and Maiti, M., *Biochem. Pharmacol.*, 1994, **48**, 2097-2102.
- Nandi, R., Chakraborty, S. and Maiti, M., *Biochemistry*, 1991, **30**, 3715-3720.
- Ray, A. and Maiti, M., *Biochemistry*, 1996, **35**, 7394-7402.
- Ray, A., Suresh Kumar, G., Das, S. and Maiti, M., *Biochemistry*, 1999, **38**, 6239-6247.
- McGhee, J. D. and von Hippel, P. H., *J. Mol. Biol.*, 1974, **86**, 469-489.
- Ray, A., Maiti, M. and Nandy, A., *Comput. Biol. Med.*, 1996, **26**, 497-503.
- Blackburn, M., in *Nucleic Acids in Chemistry and Biology* (eds Blackburn, M. and Gaitt, M.), Oxford-IRL Press Ltd., Oxford, 1990.
- Pullman, A. and Pullman, B., *Q. Rev. Biophys.*, 1981, **14**, 189-380.
- Chaires, J. B., *Biopolymers*, 1985, **24**, 403-409.
- Chakraborty, S., Nandi, R. and Maiti, M., *Biochem. Pharmacol.*, 1990, **39**, 1181-1186.
- Chow, W. I., Marky, I. A., Zaunczkowski, D. and Breslauer, K. J., *J. Biomol. Struct. Dyn.*, 1987, **5**, 345-359.

ACKNOWLEDGEMENTS. S.D. and A.S. thank UGC for the award of Senior Research Fellowship. A.B. thanks CSIR for award of Junior Research Fellowship.

Received 19 February 2000; revised accepted 28 April 2000